Dependence of exchange bias in NiFe/NiO bilayers on film thickness

José R. Fermin
Departamento de Física, Facultad de Ciencias,
Universidad del Zulia, Maracaibo, Venezuela.
Escuela de Ing. Industrial, Facultad de Ingeniería,
Universidad Rafael Urdaneta, Maracaibo, Venezuela.
e-mail: jfermin70@gmail.com

Received 7 September 2016; accepted 9 December 2016

Here we report on the effect of the ferromagnetic (FM) and antiferromagnetic (AF) films thicknesses on the exchange bias field in a FM/AF bilayer. For this, a series of NiFe(t_{NiFe})/NiO(t_{NiO}) bilayers were grown by DC magnetron sputtering onto commercial Si(001) wafers. Magneto-optical hysteresis loops were used as probes to measure the exchange-bias field, and the coercivity field, as functions of the in-plane angle, φ_H, and the films' thicknesses, t_{NiFe} and t_{NiO}. The in-plane symmetry of the exchange field and coercivity display unidirectional and uniaxial anisotropies, with angular dependences different from the simple $\cos\varphi_H$ and $cos^2\varphi_H$, respectively. These symmetries are intrinsically sensitive to the thickness of both NiFe and NiO layers. With respect to the FM layer thickness, the exchange bias and coercivity field follow the usual $1/t_{\mathrm{NiFe}}$, while the dependence on the thickness of the AF layer is more complicated, and is characterized by a critical behavior.

Keywords: Exchange-bias; unidirectional anisotropy; NiFe/NiO bilayers; magnetic biasing materials; exchange bias symmetry.

PACS: 75.30.Kz; 75.75.-c; 75.70.-i

1. Introducction

Since the discovery of the exchange anisotropy by Meiklejhon and Bean in 1956 on Co-CoO particles [1], systems consisting of a ferromagnetic (FM) material in contact with an antiferromagnetic (AF) material have attracted much attention during the last decade. The term exchange anisotropy field, H_{eb}, was coined to describe the magnetic interaction between the magnetic moments of the FM, and the magnetic moments of the AF just at the interface. The main features of these structures are a shift of the hysteresis curve along the applied field, an unusual increase in the coercivity, H_C, of the FM compared with the bulk value, rotational hysteresis, and torque curves following purely sinusoidal symmetry. More recently, ferromagnetic resonance (FMR) profiles displaying an unidirectional anisotropy superposed to the usual uniaxial symmetry, has been reported [2]. By the mid 1970's, almost all significant research on AF-FM exchange coupling was reported on materials involving monoxide magnetic particles,untilthe seminal paper by Hempstead et al in 1978 [3]. They reported that depositing γ-FeMn films onto Py films, larger loop shifts were produced, with significant ratios H_{EB}/H_C. They also noted that as the exchange anisotropy increased, no Barkhausen noise was observed, and then, higher GMR values were measured. These remarkable properties make AF/FM thin films unique candidates for applications in high density magnetic memories, and magnetic recording devices [4,5].

Experimentally, a diversity of materials and methods has been employed to investigate the exchange bias phenomenon in magnetic bilayers and nanostructures. This is because, in general, the magnetic properties of these systems are highly affected by growth conditions and sample treatment, purity of the alloys, substrate temperature, film thickness, roughness, chemical stability of the alloys, interdiffusion of atoms at the interface, etc. The most extensively studied AF/FM bilayers are those based on the antiferromagnetic compound FeMn [6], however, is in general difficult to obtain, corrodes easily, and crystallizes in different phases. Besides FeMn, other compounds such as NiO, NiMn, PtMn, IrMn, are also employed as AF layer [7-10]. This is because these materials may exhibit chemical stability, relatively simple crystalline structure, corrosion resistance, and are magnetically harder than FeMn. As FM layer, NiFe, NiFeCo, CoFe, are commonly used due to their soft magnetic properties, and because are easy to obtain [9,10]. More recently, we have proposed the amorphous FM compound $\mathrm{Fe}_{4.6}\mathrm{Co}_{70.4}\mathrm{Si}_{15}\mathrm{B}_{10}$ to be employed as an alternative material in exchange-biased heterostructures and artificial interfaces [11]. On the other hand, although several techniques are available to measure the magnetic properties of exchange-biased structures, most of the experiments are contradictory regarding the value of the exchange coupling field between the AF and the FM layer [12]. An example of this, are MOKE loops and FMR curves, which yield to inconsistent conclusions when both measures are compared, being very sensitive to the films' thickness. These discrepancies are indicative that the physical mechanisms responsible for the inter-film coupling at an AF/FM interface are yet not well understood.

The exchange coupling through an AF/FM interface is determined by the magnetic ordering, and is observed when the sample is field-cooled from a temperature above T_N, but below $T_C (T_N < T < TC)$, to a temperature $T < T_N$. If the magnetic field is applied in the temperature range $T_N < T < T_C$ the spins in the FM line-up with the field, while the spins in the AF remain paramagnetic. As the temperature is lowered to a value $T < T_N$, the spins in the AF follow the antiferromagnetic order with the spins near the AF/FM interface interacting ferromagnetically.

Another important aspect related to the physics of the exchange bias is the dependence on the thickness of the AF and FM layers, and the relation with the coercive field. Although this has been the subject of many theoretical [9,13] and experimental [14] studies in several AF/FM systems, there still exists controversy on the real origin of the phenomenology of exchange-coupled AF/FM bilayers. Two central features appear to be commonly reported in almost all investigations: (a) the dependence of the exchange bias and coercivity fields on the FM layer thickness follows the interface $1/t_{\rm FM}$ law; (b) there exist a critical AF layer thickness, below which the exchange bias field completely disappears. There is no doubt that these are mainly due to each sub-layer microstructure as long as the interface structure, which in turn, depends on the growth conditions.

The main goal of this study is to report on the dependence of the exchange bias field and coercivity in NiFe/NiO bilayers, as functions of both FM and AF films' thickness. The in-plane angle symmetry is also studied. Unlike previous reports, in which different growth conditions are used from work to work, all samples treated here were grown under same experimental conditions. For this two series of samples, NiFe(200 Å)/NiO(t_{AF}) and NiFe(t_{FM})/NiO(375 Å), were grown onto Si(001) substrates by DC magnetron sputtering. The exchange bias and coercivity were characterized by measuring the hysteresis loop shift obtained by surface magneto-optical Kerr effect (SMOKE).

2. Experiment

A first series of samples with the AF film thickness fixed at 375 Å, and FM layer thickness, t_{FM} , within the range 150-400 Å; and a second series of bilayers in which the FM film thickness was fixed at 200 Å, with AF layer thickness, t_{AF}, within the range 86-660 Å, were grown by DC magnetron sputtering onto single crystalline Si(001) substrates commercially obtained. The substrates were cleaned in ultrasound baths of acetone and methanol for 10 min each, and then dried in flowing nitrogen. The base pressure of the system prior deposition was 2.0×10^{-7} Torr. The films were deposited in a 3.0×10^{-3} Torr argon atmosphere in the sputter-up configuration with the substrate held at a distance of 9 cm from the target. The electrical power was 20 W and substrate temperature of 130°C. The NiO layer was first deposited onto the substrate using reactive sputtering of Ni, with an O_2 pressure of about $\sim$ 1 mT, and Ni deposition rate of 1.6 Å/s. Polycrystalline NiFe alloy was then grown on top of the NiO film, with simultaneous deposition of Ni and Fe with deposition rate of about 1 Å/s. As a reference, a single NiFe(200 Å)/Si(001) film was also grown. The thickness of the films was measured using a calibrated quartz crystal sensor.

The magnetization curves were measured by surface magneto-optical Kerr effect (SMOKE) in the longitudinal geometry. In this configuration, the detected signal is proportional to the magnetization parallel to the aplied magnetic

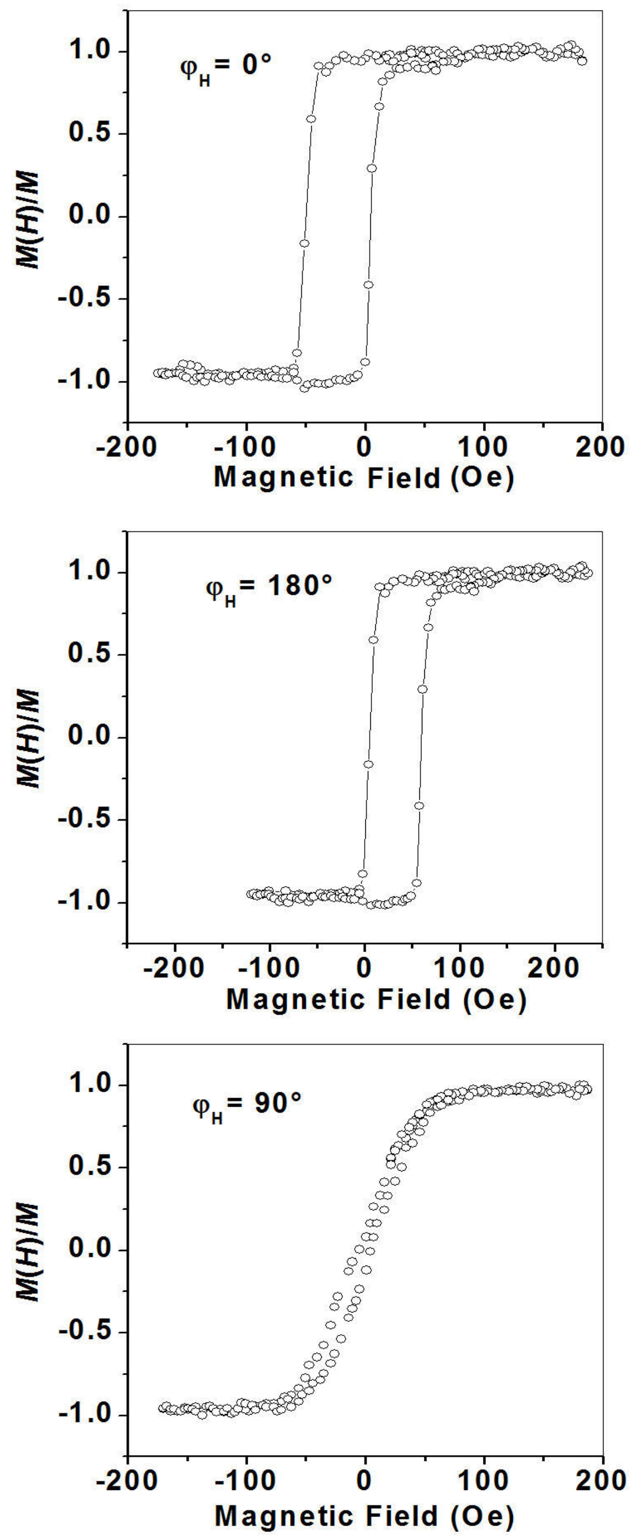

FIGURE 1. MOKE magnetization curves of NiFe(200 Å)/NiO (375 Å)/Si (001), obtained in three different orientations of the magnetic field.

field. The ligth of a 2.0 mW He-Ne laser (632.8 nm), was linearly polarized at 45° with respect to the plane of incidence, and modulated at 50 kHz by a photoelastic modulator, striking the surface of the film at an angle of incidence of about 60°. Before detection, the reflected radiation passes through an analyzer in order to select the corresponding magnetization component. In order to measure hysteris loops with respect to in-plane angle, φ_H, the sample was mounted on a goniometer that allowed us to rotate the plane of the film with respect to the applied magnetic field. From these curves we extract the values of the exchange bias field (field shift from the origin), H_{eb}, and the coercivity, H_C. All measurements were performed at room temperature.

3. Results an Discussion

The magnetization loops for the selected bilayer NiFe(200 Å)/NiO(375 Å)/Si (001), are shown in Fig. 1 for magnetic field orientations (a) $\varphi_H = 0°$, (b) $\varphi_H = 180°$, and (c) $\varphi_H = 90°$. In general, these curves are characteristic for all films' thicknesses (t_{FM} and t_{AF}), shifted from the origin, with largest field shift and maximum coercivity at $\varphi_H = 0°$, and narrow and zero-field shift at $\varphi_H = 90°$. A simple explanation of these field-shifted loops can be given by considering a phenomenological magnetic free energy in the form [14],

$$E_M(\varphi) = -MH_0 \cos\varphi + K_u \sin^2\varphi - K_{eb} \cos\varphi \quad (1)$$

where K_u is the uniaxial anisotropy constant in the FM, and K_{eb} the unidirectional anisotropy constant. The equilibrium positions of the magnetization, $\varphi = \varphi_0 = \varphi_H$, are given by the condition $\partial E_M/\partial\theta = 0$,

$$MH_0 + 2K_u \cos\varphi_0 + K_{eb} = 0. \quad (2)$$

Or equivalently,

$$\cos\varphi_H = -\frac{MH_0 + K_{eb}}{2K_u} \quad (3)$$

The exchange-bias field is obtained from Eq. (3) when H_0 equals the coercive field. In this case $M = 0$, and hence $\cos\varphi_H = -(H_{eb}/H_u)$, where $H_{eb} = K_{eb}/MS$, and $H_u = 2K_u/M_S$. This simple relation explains the most common features of the magnetization loops observed in the angle dependence of the exchange bias field and the coercivity field: $H_{EB} < 0$, $|H_{EB}| \approx H_C$, at $\varphi_H = 0°$; $H_{eb} > 0$, $H_{eb} \approx H_C$, at $\varphi_H = 180°$; and $H_{eb} = H_C = 0$, at $\varphi_H = 90°$.

From the magnetization curves the values of the exchange bias field, H_{eb}, and the coercivity shift, H_C, can be obtained as functions of the azimuthal angle, φ_H, for each series of samples. These angular dependences are shown in Fig. 2, for t_{AF} fixed at 375 Å, and with a) $t_{FM} = 160$ Å, and b) $t_{FM} = 200$ Å, and in Fig. 3 for t_{FM} fixed at 200 Å, with a) $t_{AF} = 470$ Å, and b) $t_{AF} = 568$ Å. In both series the exchange field exhibits the expected unidirectional symmetry, $H_{eb}(\varphi_H) = H_{eb}(-\varphi_H) = -H_{eb}(\pi \pm \varphi_H)$, with a period of 2π, whereas the coercivity is uniaxial, $H_C(\varphi_H) = H_C(\pi \pm \varphi_H) = H_C(\pi \pm \varphi_H)$, with a period of π. These angular dependences contain the most essential features of the exchange coupling. However, H_{eb} and H_C separately possesess additional symmetry. This additional symmetry is also present in other exchange-biased FM/AF bilayers [11, 15], and can be explained looking at the detailed form of the magnetic energy. Without loss of generality, the magnetic free energy can be considered as a series of $\cos n\varphi$,

$$E_M(\varphi) = -MH_0 \cos\varphi + \sum_{n=0} K_n \cos n\varphi,$$
$$n = 0, 1, 2, 3, \dots \quad (4)$$

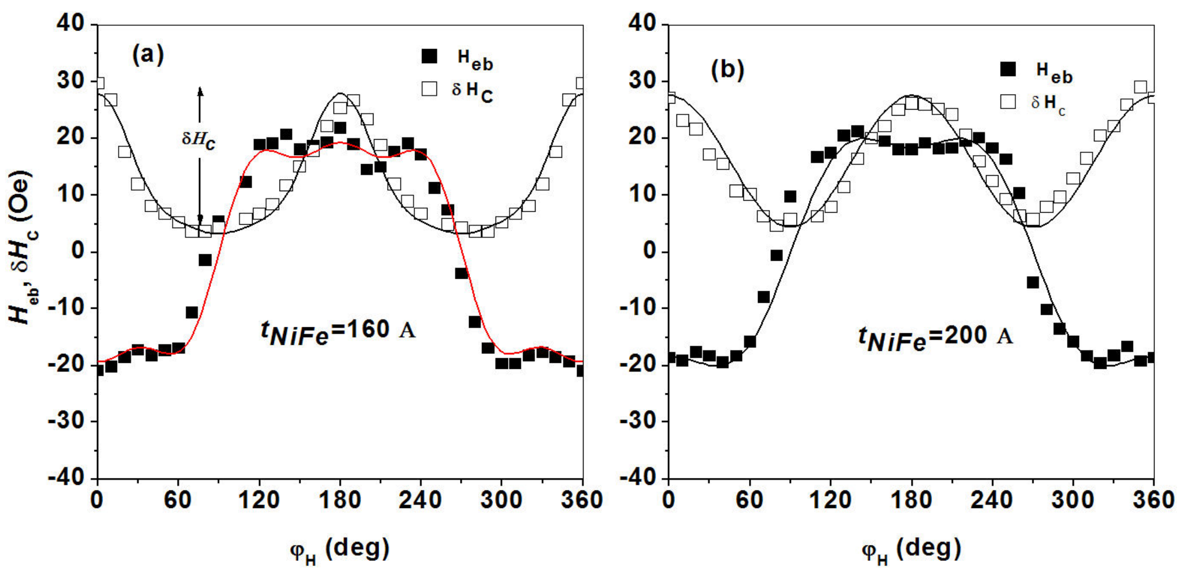

FIGURE 2. Angular dependece of coercivity, H_C, and exchange bias, H_{eb}, for (a) NiFe (160 Å)/NiO (375 Å), and (b) NiFe (200 Å)/NiO (375 Å). The solid curves are calculated from Eq. (6) using the coefficients listed in Table I.

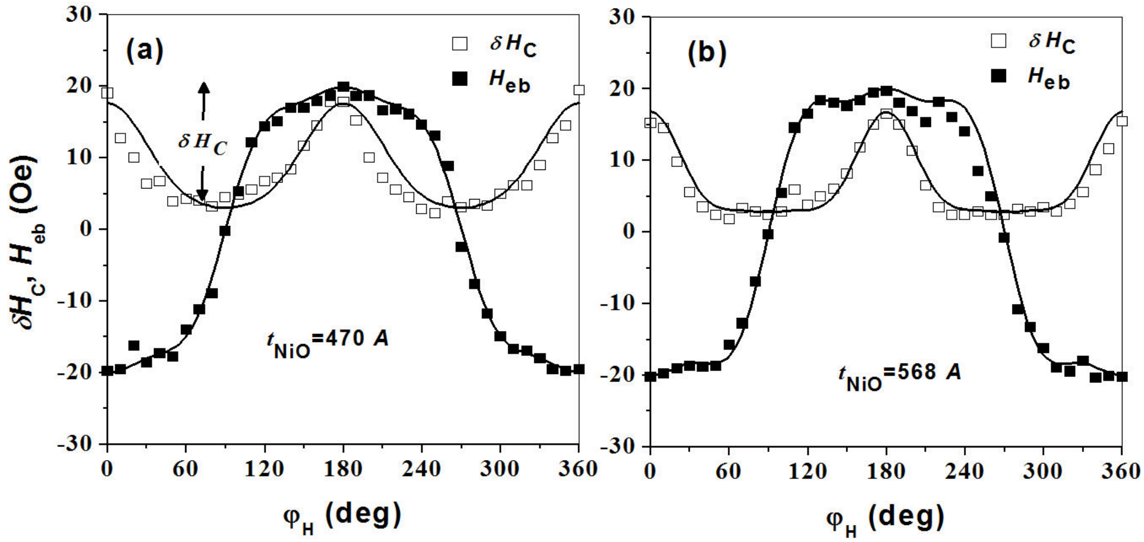

FIGURE 3. Angular dependence of coercivity, HC, and exchange bias, H_{eb}, for (a) NiFe (200 Å)/NiO (470 Å), and (b) NiFe (200 Å)/NiO (568 Å). The solid curves are calculated from Eq. (6) using the coefficients listed in Table II.

with anisotropy field, H_A,

$$H_A(\varphi) = \frac{1}{M} \sum_{n=0} K_n \cos n\varphi \tag{5}$$

which after partitioned into even-n and odd-n terms, seems like

$$H_A(\varphi) = (H_{UD,1} \cos\varphi + H_{UD,3} \cos 3\varphi + \ldots) + (H_{U,0} + H_{U,2} \cos 2\varphi + H_{U,4} \cos 4\varphi + \ldots). \tag{6}$$

One immediately recognize that the first term is unidirectional and describes the additional symmetry in the exchange-bias field, while the second is uniaxial and takes account of the additional in-plane symmetry of the coercivity. The solid curves in Figs. 2 and 3 are calculated by means of the unidirectional and uniaxial terms of Eq. (6), using the coefficients listed in Tables I and II, respectively. It is seen from Table I, that the symmetry of both H_C and H_{eb} turns simpler as the NiFe layer thickness increases, *i.e.*, less anisotropy coefficients are needed to recover the additional in-plane symmetry. On the other hand, for varying NiO layer thickness the additional symmetry still present in all samples, with anisotropy coefficients of almost the same order. The values obtained from our analysis in NiFe/NiO are very close to those reported for other FM/AF bilayers, such as amorphous FeCoSiB/NiO bilayers [11]. Numerical calculations show that the origin of these anisotropy coefficients can be related to the spin configuration at the FM/AF interface, and interface roughness [16].

An interesting property of an exchange-biased bilayer is that both the exchange-bias field shift and coercivity vary from sample to sample. This behavior gives suitable information about the interfacial nature of the magnetic anisotropies in the system. The thickness dependences of the maximum ¡field shift (measured at $\varphi_H = 180°$), and the amplitude of the coercivity curve ($\delta H_C = HC(180°) - HC(90°)$), are shown in Fig. 4 for: (a) t_{NiFe}, and (b) t_{NiO}. Both systems show a monotonic variation with respect to film thickness. However, there are some distinctive features between these two systems. As noted, the value of $H_{eb}(180°)$ and δH_C decreases gradually as the FM film thickness is increased, following the usual $1/t_{NiFe}$ law expected for all interface effects in FM thin films, as is demonstrated by the continuous curves. In contrast to these results, the dependence of $H_{eb}(180°)$ and δH_C with respect to t_{NiO} displays a more complex behavior. The solid curves in Fig. 4(b) are guides to the eye. The symbols at $t_{NiO} = 0$ represent the values of the magnetic parameters of the single NiFe film. As the thickness of the NiO layer decreases the exchange field remains constant, until a critical thickness, t_C. For $t_{NiO} < t_C$, the value of $H_{eb}(180°)$ is rapidly suppressed to zero at a minimum thickness, $t_{\text{min}} \cong 180$ Å. This critical behavior has been observed before in other FM/AF exchange-biased systems (6,9). Note that in the range of thicknesses where no exchange-bias was measured, the coercivity field is enhanced from the single film value; increasing very slowly within the range $t_{min} < t_{NiO} < t_C$; and then decreases to almost half the value of the maximum exchange field value, in the range of thicknesses $t_{NiO} > t_C$. Although the first NiO layers below t_{min} are not contributing to the exchange-bias anisotropy, these are the responsible for the onset in the uniaxial anisotropy in the FM layer.

4. Summary

NiFe/NiO exchange-biased FM/AF bilayers were deposited by DC-magnetron sputtering, onto commercial Si(100) wafers. The uniaxial and unidirectional anisotropies were

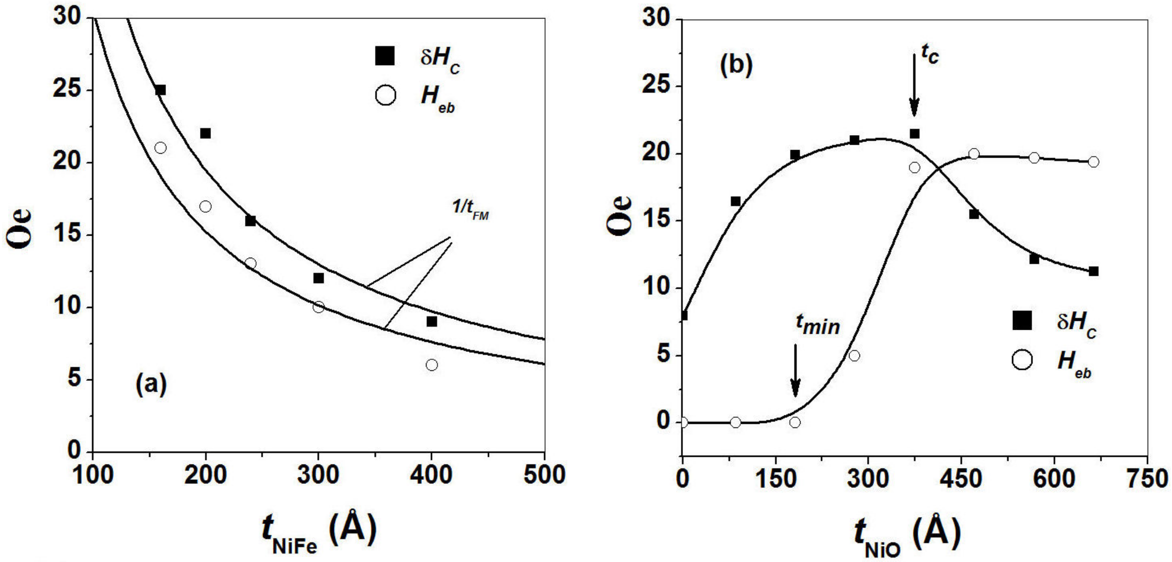

FIGURE 4. Dependence of coercivity, δH_C, and exchange bias, H_{eb}, with respect to films' thickness for (a) t_{NiFe} ; (b) t_{NiO}.

TABLE I. Anisotropy coefficients used to calculate $H_{eb}(\varphi_H)$ and $H_C(\varphi_H)$ from Eq. (6) in Fig. 2.

t_{NiFe} (Å)	H_{UD1} (Oe)	H_{UD3} (Oe)	H_{UD5} (Oe)	H_{U0} (Oe)	H_{U2} (Oe)	H_{U4} (Oe)	H_{U6} (Oe)
160 Å	-22.0	5.28	-2.64	12.0	11.40	3.60	0.96
200 Å	-23.0	4.60	—	16.0	11.60	—	—

TABLE II. Anisotropy coefficients used to calculate $H_{eb}(\varphi_H)$ and $H_C(\varphi_H)$ from Eq. (6) in Fig. 3.

t_{NiO} (Å)	H_{UD1} (Oe)	H_{UD3} (Oe)	H_{UD5} (Oe)	H_{U0} (Oe)	H_{U2} (Oe)	H_{U4} (Oe)	H_{U6} (Oe)
470 Å	-22.0	3.30	-1.21	9.0	7.20	1.35	0.09
568 Å	-23.0	4.83	-1.84	7.0	6.30	2.80	0.07

then studied using Surface Magneto-optic Kerr Effect (SMOKE), as functions of the in-plane angle, and with respect to the NiFe and NiO layer thicknesses. The exchange bias and coercivity fields exhibit in-plane unidirectional and uniaxial symmetries, with angular dependences different from the simple $\cos\varphi_H$ and $\cos^2\varphi_H$, and can be explained including higher-order terms into the magnetic anisotropy energy. The FM thickness dependence of both exchange field and coercivity follow the usual inverse thickness law, typical of purely interfacial phenomenon. With respect to the AF layer thickness, the dependence of H_{eb} and H_C display a critical behavior, characterized by two main parameters: a minimum thickness, tmin, below which there is zero exchange-bias, with a coercivity field increasing rapidly from the single FM film value as t_{NiO} increases; and a critical thickness, t_C, at which the exchange field is maximum and constant, and the coercivity falls to half the value of the maximum exchange-bias field. This critical behavior is not unique of NiFe/NiO exchange-biased bilayers but it is also present in other FM/AF systems, and might be of importance in the spin-valve head design and related spintronic devices.

Acknowledgments

The author we like to acknowledge Dr. Antonio Azevedo Costa (AAC), and Dr. Sergio M. Rezende (SMR), from the Departamento de Física, UFPE (Recife, Brazil), for supplying the samples. Special thanks to AAC for assistance in the SMOKE measurements.

1. W.H. Meiklejohn and C.P. Bean, *Phys. Rev. New magnetic anisotropy*, **102** (1956) 1413-1414.
2. S.M. Rezende, A. Azevedo, F.M. de Aguiar, M.A. Lucena, J.R. Fermin, and S.S.P. Parkin, *J. Magn. Magn. Mater*. **272-276** (2004) 321
3. R.D. Hempstead, S. Krongelb and D. A. Thompson, *IEEE Trans. Magn.* **14** (1978) 521-523.
4. S. Moyerman *et al*., *J. Appl. Phys.* **99** (2006) 08R505.
5. S. Van Dijken, M. Crofton, M. Czapkiewicz , M. Zoladz, T. Stobiecki, *J. Appl. Phys*. **99** (2006) 083901.
6. R. Jungblut et al., *J. Magn. Magn. Mater.* **148** (1995) 300-306.
7. A.E. Berkowitz, and K. Takano, *J. Magn. Magn. Mater.* **200** (1999) 552-570.
8. R.P. Michel, A. Chaiken, Y.K. Kim, and L.E. Johnson, *IEEE Transactions on Magnetics* **32** (1996) 4651-4653.
9. H. Xi, B. Bian, K.R. Mountfield, Z. Zhuang, D.E. Laughlin, R.M. White, *J. Magn. Magn. Mater.* **260** (2003) 273.
10. S.M. Rezende, M.A. Lucena, Azevedo, F.M. de Aguiar, J.R. Fermin, and S.S.P. Parkin, *J. Appl. Phys.* **93** (2003) 7717-7719.
11. J.R, Fermin, *Rev. Latin. Am. Metal. Mat.* **35** (2015) 254-258.
12. J.R. Fermin, M.A. Lucena, A. Azevedo, F.M. de Aguiar, and S.M. Rezende, *J. Appl. Phys.* **87** (2000) 6421-6423.
13. M. S. Lund *et al*., *Phys. Rev. B* **66** (2002) 054422-054422-7.
14. A.E. Berkowitz, Kentaro Takano, *J. Magn. Magn. Mater.* **200** (1999) 552-570.
15. X.W. Wu, T. Ambrose, and C.L. Chien, *J. Appl. Phys*. **72** (1998) 2176-2178.
16. J.V. Kim, L. Wee, R.L. Stamps, R. Street, *IEEE Transactions on Magnetism* **35** (1999) 2994-2997.